A kinetic discontinuous Galerkin method for the nonconservative bitemperature Euler model

Denise Aregba-Driollet, Afaf Bouharguane, Stéphane Brull

A KINETIC DISCONTINUOUS GALERKIN METHOD FOR THE NONCONSERVATIVE BITEMPERATURE EULER MODEL

DENISE AREGBA-DRIOLLET, AFAF BOUHARGUANE, AND STÉPHANE BRULL

Abstract. This paper is devoted to the construction of a discontinuous Galerkin discretisation for the nonconservative bitemperature Euler system *via* a a discrete BGK formulation. This formulation is compatible with the entropy properties of the system and thus provides admissible solutions. The DG method is used to approximate the linear transport part of the BGK model while the force and source-terms are treated implicitly but with explicit expressions. High order in time has also been investigated using SSP Runge-Kutta methods. We numerically show the good agreement of our results with the ones provided by other schemes, including solutions with shocks.

Keywords nonconservative hyperbolic system, discrete BGK approximation, discontinuous Galerkin methods, Runge-Kutta methods.

AMS subject classification 65M08, 35L60, 76X05, 35Q31

1. Introduction

This paper is devoted to the approximation of the bitemperature Euler system from a Discontinuous Galerkin (DG hereafter) method applied to a kinetic formulation proposed by Aregba and Natalini [11] and that is based on the discrete BGK model. The present fluid model is able to treat out of equilibrium regimes. The standard strategy in plasma physics, for simulating such regimes is to develop PIC methods, that directly solve the kinetic equations. But these methods are computationally very expensive. Therefore, the bitemperature model is a compromise between the precision of the kinetic models and the lower numerical cost of fluid models. This system is made of two conservation equations for mass and momentum and of two non conservative equations for ionic and electronic energies. It describes the interaction of a mixture of thermalized ions and electrons in a quasi-neutral regime. This system is nonconservative because of the presence of a relaxation source term and of products between velocity and pressure gradients. Those products make difficult the definition of weak solutions. In [20], a general framework has been developed in order to define shocks in this context by using families of paths. The generalization of this approach to a numerical setting has been considered in [25]. However, even if the path is known theoretically, the numerical determination of the path is delicate [2]. In [19], the authors consider the bitemperature Euler system with diffusive terms and by assuming that the electrons are isentropic. In that case, the system is transformed into a system of conservation laws. This approach has also been used in [27] where magnetic fields are considered and a conservation equation on electronic entropy is derived. In [13], magnetic fields are also considered in a transverse magnetic configuration. Moreover, a Suliciu scheme is derived and proved to be entropic. In [28], the authors perform a Chapman-Enskog expansion by introducing a small parameter representing the ratio between electronic and ionic molecular masses. At the end, they obtain a system with an hyperbolic part for ions and a parabolic part for electrons.

Discrete BGK schemes have been introduced in [24, 11]. The method is performed by a transport projection approach. The advantage is to put the nonlinearity inside the relaxation term whereas the transport term is linear with constant advection velocities.

More precisely, the bitemperature model under consideration is obtained in [5], by using an hydrodynamic limit starting from a BGK model coupled with Poisson and Ampère equations in a quasi-neutral regime. In particular, it is shown that the nonconservative terms come from the

Ohm's law defining the electric field. By using this asymptotic a finite volume BGK scheme has been designed in [5] by generalizing the Aregba-Natalini method [11] to a nonconservative setting. In particular, a force term is incorporated in the discrete BGK formulation in order to deal with the nonconservative terms. This formulation leads to the resolution of an hyberbolic system from a BGK relaxation process. Hence we have to deal with a linear advection term and a source term. Moreover, a Suliciu approach is developed in [5] and several comparisons are performed with different schemes. Next, in [7] the kinetic approach has been generalized to a polyatomic setting by using a kinetic model with a continuous energy variable. The bi-dimensional case has been considered in [10] and a second order finite volume scheme has been obtained. In [6], a Navier-Stokes system has been derived from a Chapman-Enskog expansion and by computing viscous terms, generalizing the model considered in [16]. However, as far as we know, there is no work on the implementation of high order methods for non-conservative bitemperature model.
For similar works, recently, in [4, 3], the authors developed a discrete BGK formulation for the compressible Euler system and next perform a RD scheme in the space variable. The time discretization is obtained by using a DeC method [1]. In [18] the authors constructed a high-order implicit palindromic discontinuous Galerkin method from kinetic-relaxation approximation for solving general hyperbolic systems of conservation laws. In [21], this approach is used to solve Maxwell's equations. The aim of the present work is to provide high order methods for the bitemperature Euler system which use a DG scheme on the discrete BGK formulation with k-th degree basis for the spacial discretization and with an order $(k+1)$-SSP-Runge-Kutta method for the time integration.

This paper is organised as follows. Section 2 introduces the bitemperature Euler system. Section 3 deals with the presentation of the discrete BGK models in the conservative and in the nonconservative case. In particular the obtention of the bitemperature model from the kinetic formulation developed in [5] is explained. In section 4, the DG method applied to the discrete BGK approximation is described. In particular, the order in time is increased in order to be consistent with the order in the space variable. Section 5 is devoted to numerical experiments. We investigate the accuracy of the proposed schemes on some examples. We also compare our methods with other existing numerical schemes. An important result is that they converge to the same solutions, even in the presence of shocks.

2. Bitemperature Euler system

Subscripts e and i respectively denote electronic and ionic quantities. We denote by ρ_e and ρ_i the electronic and ionic densities, $\rho = \rho_e + \rho_i$ the total density, m_e and m_i the related masses, c_e and c_i the mass fractions. These variables satisfy

$$\rho_e = m_e n_e = c_e \rho, \quad \rho_i = m_i n_i = c_i \rho, \quad m_e > 0, \quad m_i > 0, \quad c_e + c_i = 1. \tag{1}$$

Quasineutrality is assumed, so that the ionization ratio $Z = n_e/n_i$ is a constant. This implies that the electronic and ionic mass fractions are constant and given by

$$c_e = \frac{Z m_e}{m_i + Z m_e}, \quad c_i = \frac{m_i}{m_i + Z m_e}. \tag{2}$$

Electronic and ionic velocities u_e, u_i are assumed to be in equilibrium in the model. Hence, $u_e = u_i = u$, where u denotes mixture velocity. The pressure of each species satisfies a gamma-law with its own γ exponent :

$$p_e = (\gamma_e - 1)\rho_e \varepsilon_e = n_e k_B T_e, \quad p_i = (\gamma_i - 1)\rho_i \varepsilon_i = n_i k_B T_i, \quad \gamma_e > 1, \quad \gamma_i > 1, \tag{3}$$

where k_B is the Boltzmann constant ($k_B > 0$), ε_α and T_α represent respectively the internal specific energy and the temperature of species α for $\alpha = e, i$.

Denoting by $|\cdot|$ the euclidean norm in $\mathbb{R}^D$, the total energies for the particles are defined by

$$\mathcal{E}_\alpha = \rho_\alpha \varepsilon_\alpha + \frac{1}{2}\rho_\alpha |u|^2, \quad \alpha = e, i. \tag{4}$$

We denote by $\nu_{ei} \geq 0$ the interaction coefficient between the electronic and ionic temperatures. The model consists of two conservative equations for mass and momentum and two non-conservative equations for the energies:

$$\begin{cases} \partial_t \rho + \mathrm{div}(\rho u) = 0, \\ \partial_t(\rho u) + \mathrm{div}(\rho u \otimes u + (p_e + p_i)\mathrm{I}) = 0, \\ \partial_t \mathcal{E}_e + \mathrm{div}(u(\mathcal{E}_e + p_e)) - u \cdot \nabla (c_i p_e - c_e p_i) = \nu_{ei}(T_i - T_e), \\ \partial_t \mathcal{E}_i + \mathrm{div}(u(\mathcal{E}_i + p_i)) + u \cdot \nabla (c_i p_e - c_e p_i) = -\nu_{ei}(T_i - T_e), \end{cases} \tag{5}$$

where I represents the identity matrix in $\mathbb{R}^3$. In the following we denote

$$\mathcal{U} = (\rho, \rho u, \mathcal{E}_e, \mathcal{E}_i), \quad U_\alpha = (c_\alpha \rho, c_\alpha \rho u, \mathcal{E}_\alpha). \tag{6}$$

The system (5) is hyperbolic, diagonalisable and owns 3 eigenvalues λ_-, λ_0 (with multiplicity $D+1$ where D is the space dimension), λ_+: for any $\omega \in S^{D-1}$

$$\lambda_- = u \cdot \omega - a, \qquad \lambda_0 = u \cdot \omega, \qquad \lambda_+ = u \cdot \omega + a$$

where

$$a = \sqrt{\sum_{\alpha = e,i} \frac{\gamma_\alpha p_\alpha}{\rho}} \tag{7}$$

is the sound velocity. The fields related to $\lambda_\pm$ are genuinely nonlinear, while the field related to λ_0 is linearly degenerate.

Defining the total energy $\mathcal{E} = \mathcal{E}_e + \mathcal{E}_i$ and the total pressure $p = p_e + p_i$, one can note that if $\mathcal{U}$ is a solution of system (5) then $(\rho, \rho u, \mathcal{E})$ satisfies the following conservative system:

$$\begin{cases} \partial_t \rho + \mathrm{div}(\rho u) = 0, \\ \partial_t(\rho u) + \mathrm{div}(\rho u \otimes u + p\mathrm{I}) = 0, \\ \partial_t \mathcal{E} + \mathrm{div}(u(\mathcal{E} + p)) = 0. \end{cases} \tag{8}$$

If $\gamma_e = \gamma_i$ this is the wellknown monotemperature Euler system. But even in this case, one has to deal with one more equation to determine electronic and ionic temperatures. If $\gamma_e \neq \gamma_i$ system (8) is not closed. We want to underline the fact that in both cases, the solutions of system (5) are to be defined in the context of non-conservative equations were the product of a possibly discontinuous function with a Dirac measure appears. To give a sense to such solutions, one has to bring more physical information. In [5] we obtained solutions of (5) as hydrodynamic limits of solutions of an underlying, physically realistic BGK model. The entropy-entropy flux of species α being defined as

$$\eta_\alpha(U_\alpha) = -\frac{\rho_\alpha}{m_\alpha(\gamma_\alpha - 1)} \left[\ln\left(\frac{(\gamma_\alpha - 1)\rho_\alpha \varepsilon_\alpha}{(\rho_\alpha)^{\gamma_\alpha}} \right) + C \right], \quad Q_\alpha(U_\alpha) = \eta_\alpha(U_\alpha) u, \tag{9}$$

the total entropy-entropy flux pair for (5) is

$$\eta(\mathcal{U}) = \eta_e(U_e) + \eta_i(U_i), \qquad Q(\mathcal{U}) = \eta(\mathcal{U}) u \tag{10}$$

and we proved the following entropy inequality for these hydrodynamic limits:

$$\partial_t \eta(\mathcal{U}) + \mathrm{div} Q(\mathcal{U}) \leq -\frac{\nu_{ei}}{k_B T_i T_e}(T_i - T_e)^2. \tag{11}$$

We then defined an admissible solution of (5) as a solution satisfying this inequality.

In the following we consider the 1D version of system (5):

$$\begin{cases} \partial_t \rho + \partial_x(\rho u) = 0, \\ \partial_t(\rho u) + \partial_x(\rho u^2 + p_e + p_i) = 0, \\ \partial_t \mathcal{E}_e + \partial_x(u(\mathcal{E}_e + p_e)) - u\partial_x (c_i p_e - c_e p_i) = \nu_{ei}(T_i - T_e), \\ \partial_t \mathcal{E}_i + \partial_x(u(\mathcal{E}_i + p_i)) + u\partial_x (c_i p_e - c_e p_i) = -\nu_{ei}(T_i - T_e). \end{cases} \tag{12}$$

3. BGK models

This section is devoted to the presentation of discrete BGK models that have been introduced for system of conservation laws in [11] and then generalized to the non-conservative case in [5], [8].

3.1. Underlying kinetic (BGK) models for the conservative compressible Euler system.

We start from BGK models for the Euler monotemperature equations. Denoting

$$U = (\rho, \rho u, \mathcal{E}) \in \Omega \subset \mathbb{R}^3, \quad F(U) = (\rho u, \rho u^2 + p, u(\mathcal{E} + p)),$$

the Euler system is a system of conservation laws:

$$\partial_t U + \partial_x F(U) = 0. \tag{13}$$

We assume that $p = (\gamma - 1)(\mathcal{E} - \frac{1}{2}\rho u^2)$. We follow the framework proposed by F. Bouchut in [12]. We define a measure space $(X, d\xi)$, a real valued function a defined on X, a "maxwellian function" M from $\mathbb{R}^3 \times X$ onto $\mathbb{R}^k$, and a "moment operator" P from X to $\mathcal{L}(\mathbb{R}^k, \mathbb{R}^3)$ such that for all $U \in \Omega$:

$$\int_X P(\xi)(M(U,\xi))d\xi = U, \quad \int_X P(\xi)\left(a(\xi)M(U,\xi)\right)d\xi = F(U).$$

Let $f^\varepsilon(x,t,\xi) \in \mathbb{R}^k$ be a solution of

$$\partial_t f^\varepsilon + a(\xi)\partial_x f^\varepsilon = \frac{1}{\varepsilon}(M(U(f^\varepsilon),\xi) - f^\varepsilon),$$

with

$$U(f^\varepsilon)(x,t) = \int_X P(\xi)(f^\varepsilon(x,t,\xi))d\xi.$$

Formally if $\lim_{\varepsilon\to 0} f^\varepsilon = f$, then $f(x,t,\xi) = M(U(f)(x,t),\xi)$ and $U(f)$ is a solution of (13). In [12], conditions are given for the existence of microscopic entropies compatible with all the entropies of the macroscopic limit.

3.1.1. *Example 1: a physically realistic BGK model.* Here we set

$$X = \mathbb{R}^3, \quad \xi = v, \quad d\xi = dv, \quad a(\xi) = v_1$$

and $M(U,v) \in \mathbb{R}$ is given by

$$M(U) = \frac{n}{(2\pi k_B T/m)^{3/2}} exp(-\frac{|v-u|^2}{2k_B T/m}). \tag{14}$$

The moment operator is defined as

$$P(\xi)(M) = (m, mv_1, \frac{m|v^2|}{2})M.$$

As $f^\varepsilon(x,t,v) \in \mathbb{R}$, it is a rank one model. This model is compatible with the physical entropy of Euler system.

3.1.2. *Example 2: a discrete velocity BGK model.* Here $X = \{1,2\}$, $a(\xi) = \lambda_\xi$ with $\lambda_2 > \lambda_1$, $P(\xi) = I_d$, $k = 3$ and

$$M(U,1) = \frac{\lambda_2 U - F(U)}{\lambda_2 - \lambda_1}, \quad M(U,2) = \frac{-\lambda_1 U + F(U)}{\lambda_2 - \lambda_1},$$

see [11]. For any Euler entropy, the existence of related microscopic entropies is ensured under Liu's subcharacteristic condition, see [12]:

$$\sigma(F'(U)) \subset]\lambda_1, \lambda_2[.$$

3.2. **BGK models for the nonconservative bitemperature Euler equations.** We take a BGK model for the monotemperature Euler system (13) with $\gamma = \gamma_e$ and $\gamma = \gamma_i$. We choose

$$X_e = X_i = X, \quad a_e(\xi) = a_i(\xi) = a(\xi), \quad P_e(\xi) = P_i(\xi) = P(\xi).$$

In order to approximate the nonconservative products we define a linear operator $\mathcal{N}$ such that

$$\int_X P(\xi)(\mathcal{N}M_\alpha(U_\alpha,\xi))d_\alpha\xi = -(0,\rho_\alpha,\rho_\alpha u_\alpha).$$

In the case of example 1:

$$\mathcal{N}f = v_1\partial_{v_1}f.$$

In the case of example 2:

$$\mathcal{N}f(\xi) = \begin{pmatrix} 0 & 0 & 0 \\ -1 & 0 & 0 \\ 0 & -1 & 0 \end{pmatrix} \begin{pmatrix} f_1(\xi) \\ f_2(\xi) \\ f_3(\xi) \end{pmatrix}.$$

The equations for f_e^ε and f_i^ε are coupled with the ones for the electric field E:

$$\begin{cases} \partial_t f_e^\varepsilon + a(\xi)\partial_x f_e^\varepsilon + \dfrac{q_e}{m_e}E^\varepsilon \mathcal{N} f_e^\varepsilon = \dfrac{1}{\varepsilon}(M_e - f_e^\varepsilon) + B_{ei}(f_e^\varepsilon, f_i^\varepsilon), \\ \partial_t f_i^\varepsilon + a(\xi)\partial_x f_i^\varepsilon + \dfrac{q_i}{m_i}E^\varepsilon \mathcal{N} f_i^\varepsilon = \dfrac{1}{\varepsilon}(M_i - f_i^\varepsilon) + B_{ie}(f_e^\varepsilon, f_i^\varepsilon), \\ \partial_t E^\varepsilon = -\dfrac{1}{\varepsilon^2}\left(\dfrac{q_e}{m_e}\rho_e^\varepsilon u_e^\varepsilon + \dfrac{q_i}{m_i}\rho_i^\varepsilon u_i^\varepsilon\right), \\ \partial_x E^\varepsilon = \dfrac{1}{\varepsilon^2}\left(\dfrac{q_e}{m_e}\rho_e^\varepsilon + \dfrac{q_i}{m_i}\rho_i^\varepsilon\right). \end{cases} \tag{15}$$

The source-term $B_{\alpha\beta}$ is such that

$$\int_X P(\xi)B_{\alpha\beta}d\xi = (0,0,\nu_{ei}(T_\beta - T_\alpha)).$$

When ε tends to 0, we have formally

$$u_e = u_i = u, \quad \frac{q_e}{m_e}\rho_e + \frac{q_i}{m_i}\rho_i = 0, \quad M_\alpha(U_\alpha) = f_\alpha.$$

Quasineutrality holds: $\rho = \rho c_e = \rho c_i$ and c_e, c_i are the constants defined in (2). By taking the moments, it comes that

$$\begin{cases} \partial_t\rho_\alpha + \partial_x(\rho_\alpha u) = 0, & \alpha = e,i, \\ \partial_t(\rho_\alpha u) + \partial_x(\rho_\alpha u^2 + p_\alpha) - \dfrac{q_\alpha}{m_\alpha}E\rho_\alpha = 0, & \alpha = e,i, \\ \partial_t\mathcal{E}_e + \partial_x(u(\mathcal{E}_e + p_e)) - \dfrac{q_e}{m_e}E\rho_e u = \nu_{ei}(T_i - T_e), \\ \partial_t\mathcal{E}_i + \partial_x(u(\mathcal{E}_i + p_i)) - \dfrac{q_i}{m_i}E\rho_i u = -\nu_{ei}(T_i - T_e). \end{cases} \tag{16}$$

Considering

$$\begin{cases} \partial_t(\rho c_e u) + \partial_x(\rho c_e u^2 + p_e) - \dfrac{\rho_e q_e}{m_e}E = 0, \\ \partial_t(\rho c_i u) + \partial_x(\rho c_i u^2 + p_i) - \dfrac{\rho_i q_i}{m_i}E = 0 \end{cases}$$

leads to the expression of E

$$\frac{\rho_e q_e}{m_e}E = -\frac{\rho_i q_i}{m_i}E = c_i\partial_x p_e - c_e\partial_x p_i$$

and

$$\partial_t(\rho u) + \partial_x(\rho u^2 + p_e + p_i) = 0.$$

Hence $\mathcal{U} = (\rho, \rho u, \mathcal{E}_e, \mathcal{E}_i)$ is a solution of system (5).

Theorem 3.1. Suppose that there exists microscopic entropies for the kinetic model (15) related to the entropy η. Let $\mathcal{U}$ be a solution of the Euler bitemperature model (5) obtained by passing to the limit in (15). Then one has the entropy inequality

$$\partial_t \eta(\mathcal{U}) + \partial_x Q(\mathcal{U}) \leq -\frac{\nu_{ei}}{k_B T_i T_e}(T_i - T_e)^2.$$

We define such a solution $\mathcal{U}$ as an admissible solution.

In the case of examples 1 and 2 above, the microscopic entropies exist, see [5] for details.

4. A Discontinuous Galerkin (DG) scheme

This section is devoted to discretisation of the discrete BGK model developped in section 3. We denote Δx and Δt the space and time steps and we mesh the real line by cells $C_K = [x_{K-\frac{1}{2}}, x_{K+\frac{1}{2}}]$ with $x_{K+\frac{1}{2}} - x_{K-\frac{1}{2}} = \Delta x$. In practice an interval is considered with appropriate boundary conditions : $K \in \{1, \dots, N\}$. We also denote by P^k the space of all polynomials of degree at most k.

4.1. Preliminary.

Let us consider a transport equation

$$\partial_t f + v\partial_x f = 0 \tag{17}$$

where $v \in \mathbb{R}$ and $f(t,x,v) \in \mathbb{R}$. We look for an approximation of $f(t,\cdot,v)$ under the form $\sum_{K=1}^{N} f^K(t,x,v)$ where each $f^K(t,\cdot,v)$ has C_K as support. Let $\{\Phi_j^K,\ j = 0, \dots, k-1\}$ be a basis of polynomial functions defined on C_K. Multiplying equation (17) by Φ_i^K and integrating over C_K yields

$$\int_{C_K} \partial_t f^K(t,x,v)\Phi_i^K(x)dx - v\int_{C_K} f^K(t,x,v)(\Phi_i^K)'(x)dx + v\hat{f}_{K+\frac{1}{2}}\Phi_i^K(x_{K+\frac{1}{2}}) - v\hat{f}_{K-\frac{1}{2}}\Phi_i^K(x_{K-\frac{1}{2}}) = 0.$$

We have to choose a flux $v\hat{f}_{K+\frac{1}{2}} = h(f(x^-_{K+\frac{1}{2}}), f(x^+_{K+\frac{1}{2}}), v)$. We can set the following

$$h(f,g,v) = v\left(\frac{\lambda_2}{\lambda_2 - \lambda_1}f - \frac{\lambda_1}{\lambda_2 - \lambda_1}g\right) + \frac{\lambda_1\lambda_2}{\lambda_2 - \lambda_1}(g - f) \tag{18}$$

where $\lambda_1 \leq 0 \leq \lambda_2$.

Another choice is the upwind flux: denoting $v^+ = \max(v, 0)$, $v^- = \max(-v, 0)$

$$h(f,g,v) = v^+ f - v^- g. \tag{19}$$

Now we approximate $f^K(t,x,v)$ as

$$f^K(t,x,v) = \sum_{j=0}^{k-1} f_j^K(t,v)\Phi_j^K(x). \tag{20}$$

We obtain

$$\sum_{j=0}^{k-1} M_{ij}^K \partial_t f_j^K(t,v) - v\sum_{j=0}^{k-1} S_{ij}^K f_j^K(t,v) + v\hat{f}_{K+\frac{1}{2}}\Phi_i^K(x_{K+\frac{1}{2}}) - v\hat{f}_{K-\frac{1}{2}}\Phi_i^K(x_{K-\frac{1}{2}}) = 0$$

where we have defined two matrices M^K and S^K:

$$M_{ij}^K = \int_{C_K} \Phi_j^K \Phi_i^K dx, \quad S_{ij}^K = \int_{C_K} \Phi_j^K \left(\Phi_i^K\right)' dx.$$

Denoting $f^K = (f_0^K, \dots, f_{k-1}^K)$ we have an ordinary differential system

$$M^K \partial_t f^K(t,v) + S^K f^K(t,v) = F(t,v) \tag{21}$$

We denote $f^{n+1}(x,v) = X^{\Delta t} f^n(x,v)$ the obtained numerical scheme.

It is well-known that DG schemes may oscillate when sharp discontinuities are present in the solution. Hence in order to control these instabilities we consider a generalized slope limiters [22]. We first define the interface fluxes as

$$\begin{aligned} v^-_{j+\frac{1}{2}} &= \bar{f}^K_j - m\left(\bar{f}^K_j - f^K_j(x_{j+\frac{1}{2}}), \bar{f}^K_j - \bar{f}^K_{j-1}, \bar{f}^K_{j+1} - \bar{f}^K_j\right) \\ v^+_{j-\frac{1}{2}} &= \bar{f}^K_j + m\left(\bar{f}^K_j - f^K_j(x_{j-\frac{1}{2}}), \bar{f}^K_j - \bar{f}^K_{j-1}, \bar{f}^K_{j+1} - \bar{f}^K_j\right) \end{aligned}$$

where $\bar{f}^K_j$ is the average of f^K on C_K and where m is the minmod function limiter

$$m(a_1,a_2,a_3) = \begin{cases} s \cdot \min_j |a_j| & \text{if } s = \text{sign}(a_1) = \text{sign}(a_2) = \text{sign}(a_3) \\ 0 & \text{otherwise} \end{cases}$$

Then the generalized slope limiter technique consists in replacing f^K_j on each cell C_K with $\Lambda\Pi_h$ defined by

$$\Lambda\Pi_h(f^K_j) = \begin{cases} f^K_j & \text{if } v^+_{j-\frac{1}{2}} = f^K_j(x_{j-\frac{1}{2}}) \text{ and } v^+_{j+\frac{1}{2}} = f^K_j(x_{j+\frac{1}{2}}) \\ \bar{f}^K_j + \frac{(x-x_j)}{\Delta x/2} m(v^{(1)}_j, \bar{f}^K_{j+1} - \bar{f}^K_j, \bar{f}^K_j - \bar{f}^K_{j-1}) & \text{otherwise.} \end{cases}$$

Remark 1. *Define $U(t,x) = \int_X P(\xi)(f(t,x,\xi))d\xi$. By linearity if*

$$f(t,x,v) = \sum_{K=1}^{N} \sum_{j=0}^{k-1} f^K_j(t,v)\Phi^K_j(x)$$

then

$$U(t,x) = \sum_{K=1}^{N} \sum_{j=0}^{k-1} U^K_j(t)\Phi^K_j(x) \quad \text{with} \quad U^K_j(t) = \int_X P(\xi)(f^K_j(t,\xi))d\xi.$$

4.2. **A DG scheme for the bitemperature Euler system.** Suppose that $n \geq 0$ being fixed, we have $\mathcal{U}^n = (\rho, \rho u, \mathcal{E}_e, \mathcal{E}_i)$. We define $U^n_\alpha = (\rho_\alpha, \rho_\alpha u, \mathcal{E}_\alpha)$ with $\rho_\alpha = \rho c_\alpha$.

Step 1: projection onto equilibrium We define

$$f^n_\alpha = M_\alpha(U^n_\alpha), \quad \alpha = e, i.$$

Step 2: transport by DG method. For $\alpha = e, i$

$$f^{n+\frac{1}{2}}_\alpha = X^{\Delta t} f^n_\alpha.$$

In this case, a simple Euler explicit scheme is used to discretize the time variable. According to remark 1 we then have

$$U^{n+\frac{1}{2}}_\alpha(x) = \int_X P(\xi)(f^{n+\frac{1}{2}}_\alpha(x,\xi))d\xi = \sum_{K=1}^{N} \sum_{j=0}^{k-1} U^{K,n+\frac{1}{2}}_{\alpha,j} \Phi^K_j(x)$$

with

$$U^{K,n+\frac{1}{2}}_{\alpha,j} = \int_X P(\xi)(f^{K,n+\frac{1}{2}}_j(\xi))d\xi.$$

Step 3: force and source terms. For $\alpha = e, i$

$$f^{n+\frac{3}{4}}_\alpha = f^{n+\frac{1}{2}}_\alpha - \Delta t \frac{q_\alpha}{m_\alpha} E^{n+1} \mathcal{N} f^{n+\frac{3}{4}}_\alpha + \Delta t B_{\alpha\beta}(f^{n+\frac{3}{4}}_e, f^{n+\frac{3}{4}}_i), \quad \beta \neq \alpha$$

and

$$U_\alpha^{n+1} = \int_X P(\xi)(f_\alpha^{n+\frac{3}{4}}(\xi))d\xi = (\rho_\alpha^{n+1}, \rho_\alpha^{n+1}u_\alpha^{n+1}, \mathcal{E}_\alpha^{n+1}).$$

We obtain

$$U_\alpha^{n+1} = U_\alpha^{n+\frac{1}{2}} - \Delta t \frac{q_\alpha}{m_\alpha} E^{n+1}\mathcal{N}U_\alpha^{n+1} + S(T_e^{n+1}, T_i^{n+1}).$$

Step 4: coupling with Maxwell-Ampère and Poisson equations.

$$\begin{cases} \frac{q_e}{m_e}\rho_e^{n+1} + \frac{q_i}{m_i}\rho_i^{n+1} = 0, \\ \frac{q_e}{m_e}\rho_e^{n+1}u_e^{n+1} + \frac{q_i}{m_i}\rho_i^{n+1}u_i^{n+1} = 0. \end{cases}$$

Hence $u_i^{n+1} = u_e^{n+1}$. We set $\rho^{n+1} = \rho_e^{n+1} + \rho_i^{n+1}$, $u^{n+1} = u_i^{n+1} = u_e^{n+1}$. As $q_e = -e$ and $q_i = Ze$, we get as in the continuous case $\rho_e^{n+1} = c_e\rho^{n+1}$, $\rho_i^{n+1} = c_i\rho^{n+1}$. We have analogously to (16)

$$\begin{cases} \rho_\alpha^{n+1} = \rho_\alpha^{n+\frac{1}{2}}, & \alpha = e, i, \\ \rho_e^{n+1}u^{n+1} = \rho_e^{n+\frac{1}{2}}u_e^{n+\frac{1}{2}} + \Delta t \frac{q_e}{m_e}E^{n+1}\rho_e^{n+1}, \\ \rho_i^{n+1}u^{n+1} = \rho_i^{n+\frac{1}{2}}u_i^{n+\frac{1}{2}} + \Delta t \frac{q_i}{m_i}E^{n+1}\rho_i^{n+1}, \\ \mathcal{E}_e^{n+1} = \mathcal{E}_e^{n+\frac{1}{2}} + \Delta t \frac{q_e}{m_e}E^{n+1}\rho_e^{n+1}u^{n+1} + \Delta t\nu_{ei}(T_i^{n+1} - T_e^{n+1}), \\ \mathcal{E}_i^{n+1} = \mathcal{E}_i^{n+\frac{1}{2}} + \Delta t \frac{q_i}{m_i}E^{n+1}\rho_i^{n+1}u^{n+1} - \Delta t\nu_{ei}(T_i^{n+1} - T_e^{n+1}). \end{cases} \tag{22}$$

The equations on mass and momentum give ρ^{n+1} and u^{n+1}:

$$\begin{cases} \rho^{n+1} = \rho^{n+\frac{1}{2}}, \\ \rho^{n+1}u^{n+1} = \rho_e^{n+\frac{1}{2}}u_e^{n+\frac{1}{2}} + \rho_i^{n+\frac{1}{2}}u_i^{n+\frac{1}{2}}. \end{cases} \tag{23}$$

We then compute E^{n+1} as in the continuous case:

$$c_e\rho^{n+1}u^{n+1} = \rho_e^{n+\frac{1}{2}}u_e^{n+\frac{1}{2}} + \Delta t \frac{q_e}{m_e}E^{n+1}\rho^{n+1}c_e,$$
$$c_i\rho^{n+1}u^{n+1} = \rho_i^{n+\frac{1}{2}}u_i^{n+\frac{1}{2}} + \Delta t \frac{q_i}{m_i}E^{n+1}\rho^{n+1}c_i,$$

hence

$$\Delta t \frac{q_e}{m_e}E^{n+1}\rho_e^{n+1} = -\Delta t \frac{q_i}{m_i}E^{n+1}\rho_i^{n+1} = -c_i\rho_e^{n+\frac{1}{2}}u_e^{n+\frac{1}{2}} + c_e\rho_i^{n+\frac{1}{2}}u_i^{n+\frac{1}{2}}$$

and

$$\begin{cases} \mathcal{E}_e^{n+1} = \mathcal{E}_e^{n+\frac{1}{2}} + u^{n+1}\left(-c_i\rho_e^{n+\frac{1}{2}}u_e^{n+\frac{1}{2}} + c_e\rho_i^{n+\frac{1}{2}}u_i^{n+\frac{1}{2}}\right) + \Delta t\nu_{ei}(T_i^{n+1} - T_e^{n+1}) \\ \mathcal{E}_i^{n+1} = \mathcal{E}_i^{n+\frac{1}{2}} + u^{n+1}\left(c_i\rho_e^{n+\frac{1}{2}}u_e^{n+\frac{1}{2}} - c_e\rho_i^{n+\frac{1}{2}}u_i^{n+\frac{1}{2}}\right) + \Delta t\nu_{ei}(T_e^{n+1} - T_i^{n+1}). \end{cases} \tag{24}$$

As

$$T_\alpha^{n+1} = \left(\frac{\mathcal{E}_\alpha^{n+1}}{\rho_\alpha^{n+1}} - \frac{1}{2}(u^{n+1})^2\right)\frac{(\gamma_\alpha - 1)m_\alpha}{k_B}$$

system (24) can be solved explicitly. Finally we obtain $\mathcal{U}^{n+1}(x)$, an approximation of $\mathcal{U}(t_{n+1}, x)$.

4.3. **Higher order in time.** The scheme described in subsection 4.2 can be viewed as a fractional step method which computes the approximate solution $\mathcal{U}_h^{n+1}$ at time t_{n+1} as a function of $\mathcal{U}_h^n$:

$$\mathcal{U}^{n+1} = \mathbf{E}_{\Delta t}(\mathcal{U}^n). \tag{25}$$

This method is only first order in time, even if each step is high order, basically because in the underlying Trotter formula, when two operators A and B do not commute, $\exp(\Delta t(A+B)) = \exp(\Delta tA)\exp(\Delta tB) + O(\Delta t^2)$. We can view this procedure as an explicit RK1 Euler scheme applied to the semi-discretized system obtained by performing the DG spacial discretization of system (5):

$$\partial_t \mathcal{U}_h = \mathbf{G}(\mathcal{U}_h).$$

It is important to increase the order in time when one increases the order in space, otherwise you will not observe any significant improvement of the numerical results, see section 5 below. For this purpose, we use higher order N steps explicit Runge Kutta schemes. The approximate solution $\mathcal{U}_h^n$ being known, we set

$$Y_1 = \mathcal{U}_h^n, \quad V_1 = Y_1\,, \quad \begin{cases} Y_{i+1} = \mathbf{E}_{\Delta t}(V_i), \\ V_{i+1} = d_{i1}^{(N)}\mathcal{U}_h^n + d_{i2}^{(N)} Y_{i+1}, \end{cases} \quad i = 1, \dots, N, \tag{26}$$

and

$$\mathcal{U}_h^{n+1} = V_{N+1}. \tag{27}$$

The scheme is defined by a $N \times 2$ matrix $D^{(N)} = \left(d_{ij}^{(N)}\right)$. Here we set:

$$D^{(1)} = (0,1)\,, \quad D^{(2)} = \begin{pmatrix} 0 & 1 \\ \frac{1}{2} & \frac{1}{2} \end{pmatrix}, \quad D^{(3)} = \begin{pmatrix} 0 & 1 \\ \frac{3}{4} & \frac{1}{4} \\ \frac{1}{3} & \frac{2}{3} \end{pmatrix}.$$

The case $N = 1$ is the explicit Euler method. It is used with a P^0-DG discretization. The case $N = 2$ is the RK2 Heun method, used with a P^1 DG discretization. This method is Strong Stability Preserving (SSP) [23]. For the third-order $N = 3$, we consider the Shu-Osher RK3-SSP scheme [22], used with P^2-DG discretization. It is to be noted that the case $N = 2$ can also be viewed as a DeC method [1].

We consider here the following CFL condition:

$$CFL = \frac{\Delta t}{\Delta x}|v| \leq \frac{1}{2k+1}$$

where k is the degree of the polynomial [17].

5. Numerical results

This section is devoted to the numerical validation of the numerical scheme that is constructed in the previous section. The numerical method is firstly applied to the compressible Euler system (8) and next to the bitemperature Euler system (5).

5.1. **Compressible Euler system.**

5.1.1. *Euler isentropic.* In this subsection we test the convergence of the scheme for Euler equations (8) by considering the case of isentropic flow i.e when $\gamma = 3$ and $p = \rho^\gamma$, with the initial conditions

$$\begin{pmatrix} \rho_0 \\ u_0 \\ p_0 \end{pmatrix} = \begin{pmatrix} 1 + 0.5\sin(\pi x) \\ 0 \\ \rho_0^\gamma \end{pmatrix}$$

where the domain is $\Omega = [-1, 1]$, the final time $T = 0.1$ and we take $CFL = 0.1$. We plot in Figure 1 the numerical order of convergence of the method. The considered error is the L^2-norm.

We observe that we get $k+1$ order when we choose a P^k-DG discretisation the space with a time discretisation of order $k+1$.

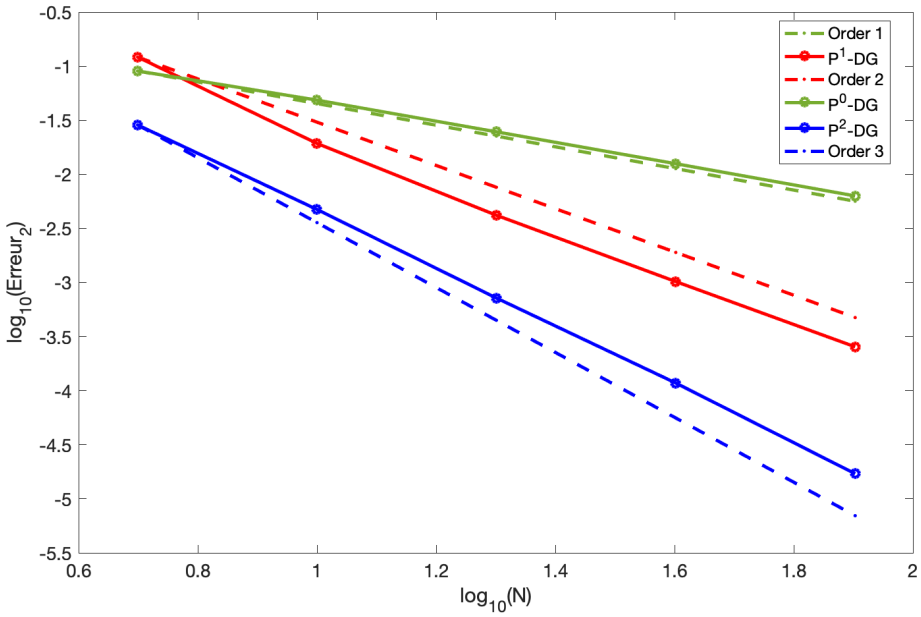

FIGURE 1. Convergence of u for Euler equations

5.1.2. *Shu-Osher test case.* We consider the test case [26] applied to the compressible Euler system for $\gamma = 1.4$. The initial conditions of the Shu-Osher test are given by

$$\begin{pmatrix}\rho_0\\ u_0\\ p_0\end{pmatrix} = \begin{pmatrix}3.857143\\ 2.6929369\\ 10.333333\end{pmatrix} \text{ if x} \in [-5,-4], \quad \begin{pmatrix}\rho_0\\ u_0\\ p_0\end{pmatrix} = \begin{pmatrix}1+0.2\sin(5x)\\ 0\\ 1\end{pmatrix} \text{ if x} \in [-4,5],$$

on the domain $[-5, 5]$ and the final time of the problem is $T = 1.8$.

The reference solution represented in Figure 2 is obtained with the P^2-DG method with 5000 points. We compare in Figure 2 the results obtained with the P^0, the P^1 and the P^2 method for 512 points with the reference solution. We observe that the oscillations are well captured by the P^2 reconstruction and that the precision increases with the order of the scheme.

5.1.3. *Blast waves.* In order to highlight the advantages for using a high order method, we consider the test case proposed by Collela and Woodward [15] devoted to the compressible Euler system for $\gamma = 1.4$. We consider the initial conditions $\rho_0 = 1$, $u_0 = 0$, $p_0 = 10^3\mathbb{1}_{[0,0.1[} + 10^{-2}\mathbb{1}_{[0.1,0.9[} + 10^2\mathbb{1}_{[0.9,1]}$. The density and the energy are displayed in Figure 3 for 1000 points in space. As observed in Figure 3, the P^2 reconstruction is able to catch correctly the second pick.

All the previous numerical tests have been tested in [4] for a RD scheme and analogous results are obtained.

5.2. **Bitemperature Euler system.** Next the numerical method is applied to the bitemperature Euler system (12). In 5.2.1, we perform a convergence study for the DG kinetic scheme for the P^1 and the P^2 reconstruction. In the next test cases, the DG kinetic scheme for the P^2 reconstruction is compared with the kinetic scheme for a finite volume space discretization (FV kinetic scheme) and the Suliciu method developed in [5].

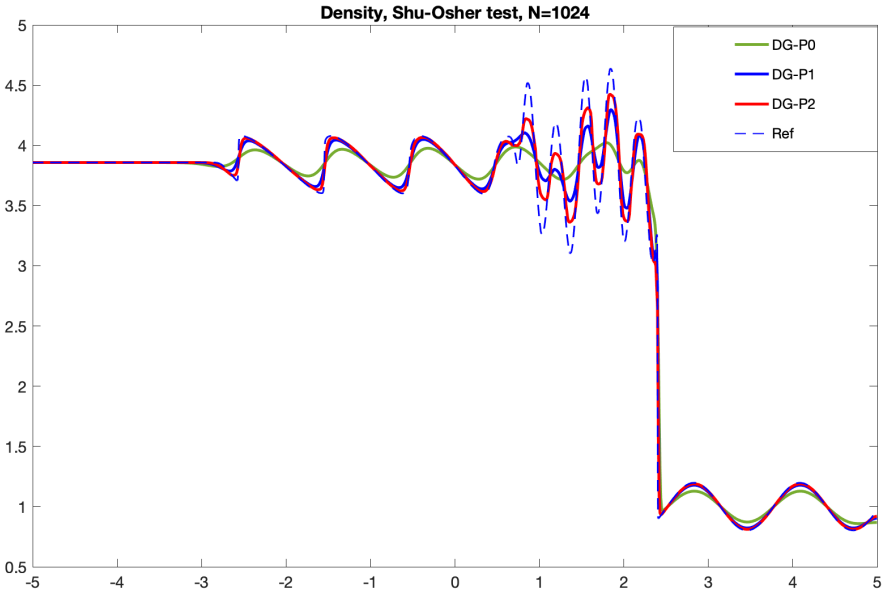

FIGURE 2. Density for the Shu-Osher test case.

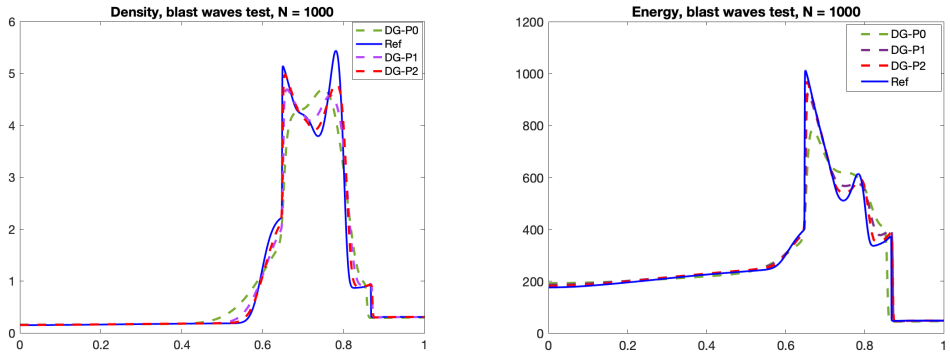

FIGURE 3. Density (left) and Energy (right) for the blast waves.

5.2.1. *Analytical test case.* We look for a smooth analytical solution of system (12). We assume that ρ and u are constant, so that the system reduces to

$$\begin{cases} \partial_x(ZT_e + T_i) = 0, \\ \partial_t T_e + u\partial_x T_e = \beta_e(T_i - T_e), \\ \partial_t T_i + u\partial_x T_i = \beta_i(T_e - T_i) \end{cases} \tag{28}$$

with

$$\beta_\alpha = \frac{\nu_{ei} m_\alpha(\gamma_\alpha - 1)}{\rho c_\alpha k_B}, \quad \alpha \in \{e, i\}.$$

We choose initial temperatures $T_e(x,0) = T_{e,0}(x)$, $T_i(x,0) = T_{i,0}(x)$ such that

$$\partial_x(ZT_{e,0} + T_{i,0}) = 0. \tag{29}$$

It is easy to compute the solution (T_e, T_i) of the last two equations: denoting $\beta_1 + \beta_2 = \beta$, $\mu = \frac{\gamma_e - 1}{Z} + \gamma_i - 1$:

$$(30)\quad \begin{cases} T_e(x+ut,t) &= \dfrac{1}{\mu}\left(\dfrac{\gamma_e-1}{Z}(T_{e,0}(x)-T_{i,0}(x))\mathrm{e}^{-\beta t} + (\gamma_i-1)T_{e,0}(x) + \dfrac{\gamma_e-1}{Z}T_{i,0}(x)\right), \\ T_i(x+ut,t) &= \dfrac{1}{\mu}\left((\gamma_i-1)(T_{i,0}(x)-T_{e,0}(x))\mathrm{e}^{-\beta t} + (\gamma_i-1)T_{e,0}(x) + \dfrac{\gamma_e-1}{Z}T_{i,0}(x)\right). \end{cases}$$

Then one can observe that if $\gamma_e \neq \gamma_i$ the first equation of (28) cannot be satisfied unless $\partial_x T_{e,0} = \partial_x T_{i,0} = 0$. Therefore we set $\gamma_e = \gamma_i$. In that case, if (29) is satisfied then (30) gives a solution of the bitemperature Euler system.

We choose $\nu_{ei} = 1$, $T = 0.1$, $\Omega = [0,1]$ and $CFL = 0.1$. We plot in Figure 4 the convergence of the method for the bitemperature Euler system (12). In contrast to compressible Euler system, the numerical simulation show a convergence of order k when using a P^k-DG for the space discretisation and with a $(k+1)$-SSP-RK time approximation.

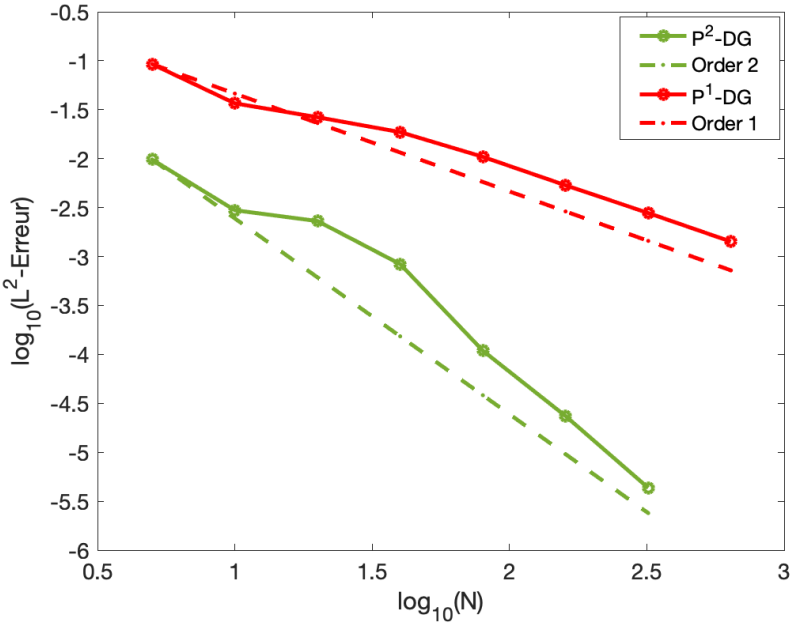

FIGURE 4. Convergence of electronic temperature for the bitemperature Euler system

5.2.2. *Double shock.* In this test case, we consider the following physical parameters:

$$k_B = 1.3807 \times 10^{-23}\ \mathrm{J.K}^{-1}, \quad m_e = 9,1094 \times 10^{-31}\ \mathrm{kg}, \quad m_i = 1.6726 \times 10^{-27}\ \mathrm{kg},$$
$$e = -q_e = q_i = 1.6022 \times 10^{-19}\ \mathrm{C}, \quad \gamma_e = \frac{5}{3}, \quad \gamma_i = \frac{7}{5}.$$

We consider a double shock for $\nu_{ei} = 0$ which is a Riemann problem

$$\rho_L = 1, \quad u_L = 10^5, \quad T_{e,L} = 2.3\,10^7, \quad T_{i,L} = 2.3\,10^6$$
$$\rho_R = 1, \quad u_R = -10^5, \quad T_{e,R} = 2.3\,10^7, \quad T_{i,R} = 2.3\,10^6.$$

The results for electronic and ionic temperatures are displayed in fig. 5 and 6 at time $t = 4.09\,10^{-7}$ s for 10000 points in space. They are obtained with the Suliciu method, the finite volume kinetic

method constructed in [5] and the DG method with a P^2 reconstruction developed in this paper. The three methods show analogous results.

5.2.3. *Double rarefaction wave.* Using similar physical parameters as in subsection 5.2.2 we consider here a rarefaction wave for $\nu_{ei} = 0$ which is a Rieman problem

$$\rho_L = 1, \quad u_L = -10^5, \quad T_{e,L} = 2.3\,10^7, \quad T_{i,L} = 2.3\,10^6,$$
$$\rho_R = 1, \quad u_R = 10^5, \quad T_{e,R} = 2.3\,10^7, \quad T_{i,R} = 2.3\,10^6.$$

We take $\gamma_e = 5/3$ and $\gamma_i = 7/5$. This test case is a rarefaction wave computed at time $t = 4.09\,10^{-7}$ s for 10000 points in space. In this test case, an analytical solution can be computed. The results displayed in Figure 7 and in Figure 8 compare for electronic and ionic temperatures the P^2 reconstruction with the finite volume kinetic scheme and the Suliciu scheme developed in [5]. All the scheme show a good agreement with the exact solution.

5.2.4. *Stationary shock.* We consider here the test case of the stationary shock presented in [5] in the case $\nu_{ei} = 100$ and with the following parameters:

$$k_B = 1.0, \quad m_e = 10^{-3}, \quad m_i = 1.0, \quad Z = 1.0, \quad \gamma_e = \gamma_i = 5/3 \tag{31}$$

In that case, the left and the right states of the Riemann problem are the following

$$\rho_L = 1.001, \quad u_L = 10, \quad T_{e,L} = 1, \quad T_{i,R} = 1,$$
$$\rho_R = 3.640330609, \quad u_R = 2.749750250, \quad T_{e,R} = 3, \quad T_{i,R} = 17.5060240977.$$

The results displayed in Figure 9 and in Figure 10 are computed for 10000 points in space and at time $t = 0.005s$.

5.2.5. *Sod test case.* We finally consider the test case of the sod test case in with the parameters (31), $\nu_{ei} = 0$ and a final time $0.05\,s$

$$\rho_L = 1, \quad u_L = 0, \quad T_{e,L} = 1, \quad T_{i,R} = 1,$$
$$\rho_R = 0.125, \quad u_R = 0, \quad T_{e,R} = 2, \quad T_{i,R} = 3.$$

Figures 12 and 11 represent ionic and electronic temperatures for 10000 points in space with Suliciu, kinetic and discontinuous Galerkin method with a P^2 reconstruction. The three schemes show the same results. In particular, the "plateaux" after the shocks have the same amplitude. The DG kinetic scheme shows some oscillations for the electronic temperatures. However, these oscillations do not propagate.

6. Conclusion and perspectives

In this paper, we have developed a DG-kinetic scheme for the bitemperature Euler system for different order of space discretization. The principle is to consider a discrete BGK model as in [5] and to construct a DG discretisation with k-th degree basis for the space discretization and with an $(k+1)$-SSP-Runge-Kutta method for the time discretization. Due to the kinetic model, a special treatment has been used to implement the order in time. This method has been illustrated on several test cases and numerical order have been investigated on both conservative Euler equations and on nonconservative bitemperature Euler model. It is to be noted that in the nonconservative case, when shocks occur, the electronic and ionic temperatures cannot be predicted analytically, even in the framework of a Riemann problem as for a conservative system. They can depend on the numerical viscosity. A crucial fact here is that even in the presence of shocks we observe that whatever the order, the DG method converges to the same solutions as the ones obtained in previous articles.

The generalization of the present work to a two dimensional framework as done in [10] for finite volumes is postponed to a future paper. Moreover in the present case, only the electric field has been taken into account. The question of the presence of the magnetic fields can also be considered as in [14] for a transverse magnetic field.

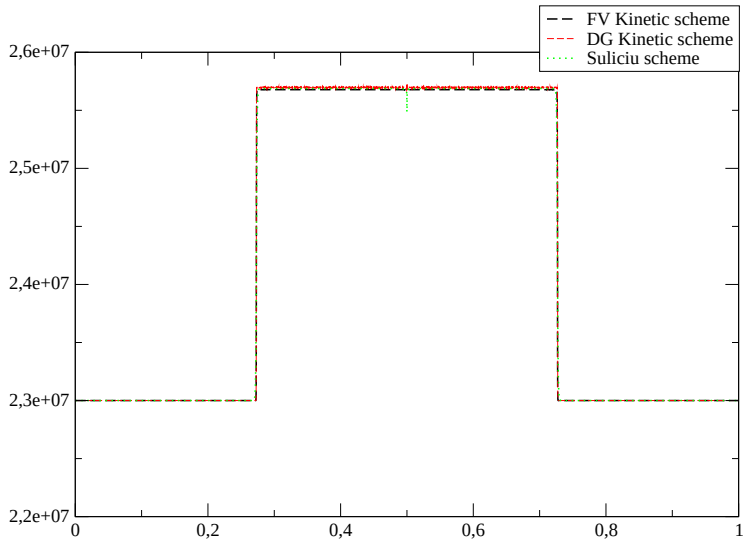

FIGURE 5. Electronic temperature for the double shock computed with the DG kinetic scheme, the finite volume kinetic scheme, the Suliciu scheme, with 10000 points in space

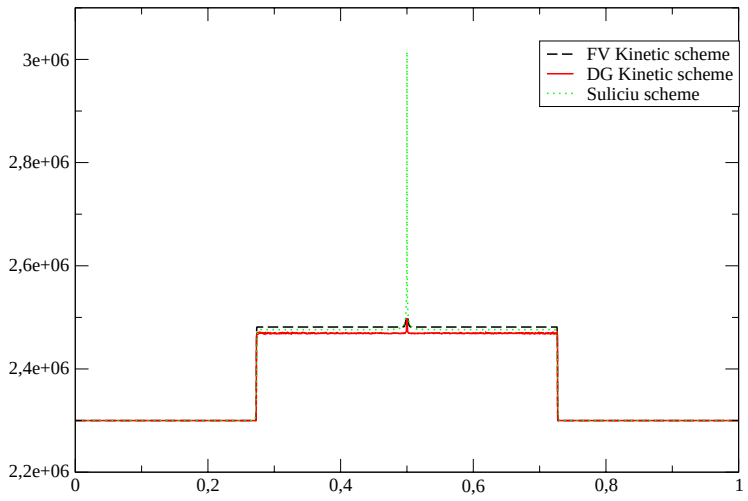

FIGURE 6. Ionic temperature for the double shock computed with the DG kinetic scheme for a P^2 reconstruction, the finite volume kinetic scheme, the Suliciu scheme, with 10000 points in space

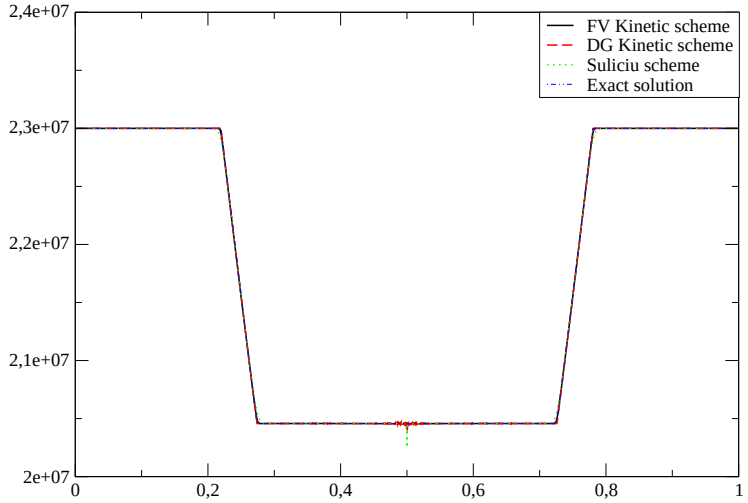

FIGURE 7. Electronic temperature for the double rarefaction wave computed with the DG scheme for a P^2 reconstruction, the kinetic scheme, the Suliciu scheme and the exact solution

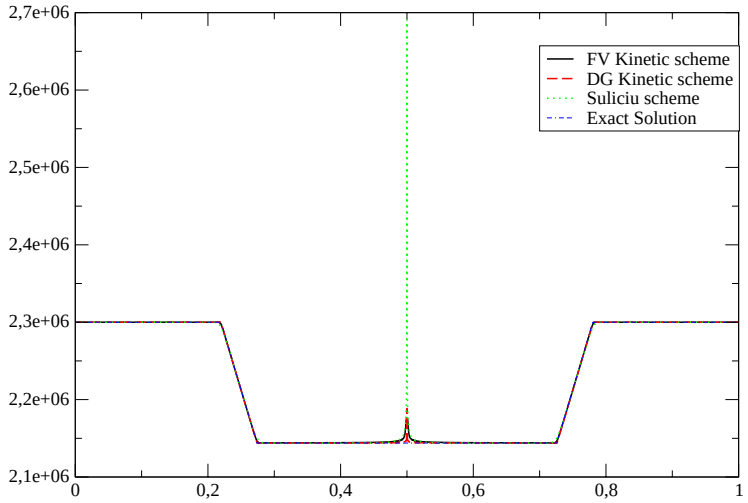

FIGURE 8. Ionic temperature for the double rarefaction computed with the DG kinetic scheme, the finite volume kinetic scheme, the Suliciu scheme and the exact solution

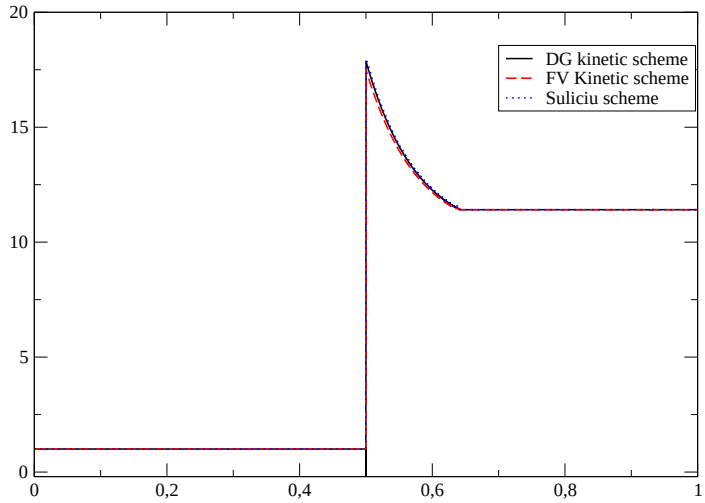

FIGURE 9. Ionic temperature for the stationary shock computed with the DG kinetic scheme, the finite volume kinetic scheme, the Suliciu scheme.

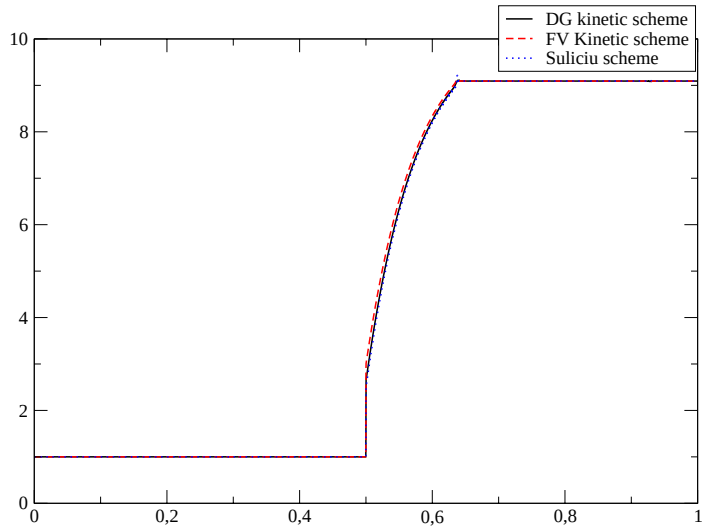

FIGURE 10. Electronic temperature for the stationary choc computed with the DG kinetic scheme, the finite volume kinetic scheme, the Suliciu scheme

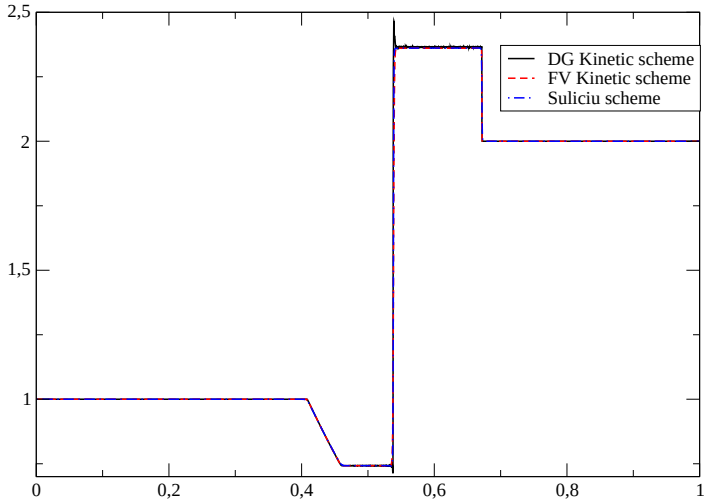

FIGURE 11. Electronic temperature for the sod test case computed with the DG kinetic scheme, the finite volume kinetic scheme, the Suliciu scheme computed with 10000 points.

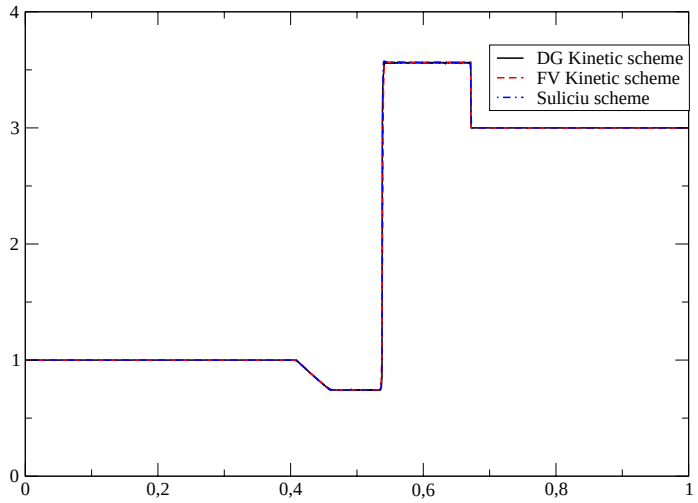

FIGURE 12. Ionic temperature for sod test case computed with the DG kinetic scheme, the finite volume kinetic scheme, the Suliciu scheme computed with 10000 points

References

[1] R. Abgrall High order schemes for hyperbolic problems using globally continous approximation and avoiding mass matrices *Journ. Sci. Comput.* 73, 461-494, 2017

[2] R. Abgrall and S. Karni, A comment on the computation of non-conservative products, *Journal of Computational Physics*, 229 (2010), pp. 2759–2763.

[3] R. Abgrall and D. Torlo. Some preliminary results on high order asymptotic preserving computationally explicit kinetic scheme *Comm Maths Sci.*, 20(2):297–326, 2022.

[4] R. Abgrall and D. Torlo. High order preserving deferred correction implicit-explicit schemes for kinetic models. *Siam journal of scientific computing*, 42(3):816–845, 2020.

[5] D. Aregba–Driollet, J. Breil, S. Brull, B. Dubroca, and E. Estibals. Modelling and numerical approximation for the nonconservative bitemperature Euler model. *ESAIM: Mathematical Modelling and Numerical Analysis*, 52(4):1353–1383, 2018.

[6] D. Aregba-Driollet and S. Brull. About viscous approximations of the bitemperature euler system. *Communications in Math Sciences*, 17(4):1135–1147, 2019.

[7] D. Aregba-Driollet and S. Brull. Modelling and numerical study of the polyatomic bitemperature euler system. Netw. Heterog. Media 17 (2022), no. 4, 593–.

[8] D. Aregba-Driollet, S. Brull, and X. Lhébrard. Nonconservative hyperbolic systems in fluid mechanics. In *SMAI 2017—8ème Biennale Française des Mathématiques Appliquées et Industrielles*, volume 64 of *ESAIM Proc. Surveys*. EDP Sci., 2018.

[9] D. Aregba-Driollet, S. Brull and Y.-J. Peng, Global existence of smooth solutions for a non-conservative bitemperature Euler model, *SIAM J. Math. Anal.* 53 (2021), no. 2, 1886-1907.

[10] D. Aregba-Driollet, S. Brull and C. Prigent, A discrete velocity numerical scheme for the two-dimensional bitemperature Euler system, *SIAM J. Numer. Anal.* 60 (2022), no. 1, 28-51.

[11] D. Aregba-Driollet and R. Natalini. Discrete kinetic schemes for multidimensional systems of conservation laws. *SIAM Journal on Numerical Analysis*, 37(6):1973–2004, 2000.

[12] F. Bouchut. Construction of BGK Models with a Family of Kinetic Entropies for a Given System of Conservation Laws. *Journal of Statistical Physics*, 95:113–170, 1999.

[13] S.Brull, B.Dubroca, and X.Lhébrard Modelling and entropy satisfying relaxation scheme for the nonconservative bitemperature Euler system with transverse magnetic field, *Computers and Fluids*, 214, (2021)

[14] S. Brull, B. Dubroca, and C. Prigent. A kinetic approach of the bi-temperature Euler model, *Kinetic & Related Models*, 13 1, 33–61, 2020

[15] P. Collela and Woodward. The piecewse parabolic method (PPM) for gas dynamical simulations. *Journal of Computational Physics*, 54:174–201, 1984.

[16] C. Chalons, F. Coquel Navier-Stokes equations with several independant pressure laws and explicit predictor-corrector schemes *Numerische Math. 103, 3 (2005), 451-478*

[17] Cockburn, B., Shu, CW. Runge–Kutta Discontinuous Galerkin Methods for Convection-Dominated Problems. *Journal of Scientific Computing* 16, 173–261 (2001).

[18] D. Coulette, E. Franck, P. Helluy, M. Mehrenberger, L. Navoret, High-order implicit palindromic discontinuous Galerkin method for kinetic-relaxation approximation, *Computers & Fluids* , Volume 190, 2019

[19] F. Coquel and C. Marmignon, Numerical methods for weakly ionized gas, *Astrophysics and Space Science*, 260 (1998), pp. 15–27.

[20] G. Dal Maso, P. Le Floch, and F. Murat, Definition and weak stability of nonconservative products, *Journal de mathématiques pures et appliquées*, 74 (1995), pp. 483–548.

[21] P. Gerhard, P. Helluy and V. Michel-Dansac Unconditionally stable and parallel Discontinuous Galerkin solver. *Computers and Mathematics with Applications, 112:116–137, 2022*

[22] J. S. Hesthaven, and T. Warburton, Nodal Discontinuous Galerkin Methods: Algorithms, Analysis, and Applications, Springer Publishing Company, Incorporated *(2007)*

*[23] Isherwood, Leah, Grant, Zachary J. and Gottlieb, Sigal Strong stability preserving integrating factor Runge-Kutta methods SIAM J. Numer. Anal., **56**, 3276–3307 (2018).*

[24] R. Natalini, A discrete kinetic approximation of entropy solutions to multidimensional scalar conservation laws. J. Differential Equations, 148, no. 2, 292–317, (1998)

[25] C. Parés, Path-conservative numerical methods for nonconservative hyperbolic systems, in Numerical methods for balance laws, vol. 24 of Quad. Mat., Dept. Math.*, Seconda Univ. Napoli, Caserta, 2009, pp. 67–121.*

[26] C. W. Shu and S. Osher, Efficient implementation of essentially non-oscillatory shock-capturing schemes Journal of Computational Physics*, Volume 77, Issue 2.*

[27] A. Sangam, E. Estibals and Guillard, Derivation and numerical approximation of two-temperature Euler plasma model. J. Comput. Phys. *444 (2021),*

[28] Q. Wargnier, S. Faure, B. Graille, T. Magin, and M. Massot, Numerical treatment of the nonconservative product in a multiscale fluid model for plasmas in thermal nonequilibrium: application to solar physics, SIAM. J. Sci. Comput.*, 42 (2020), pp. 1–27.*

Univ. Bordeaux, CNRS, Bordeaux INP, IMB, UMR 5251, F-33400 Talence, France
Email address: denise.aregba@math.u-bordeaux.fr

Univ. Bordeaux, Institut de Mathématiquesde Bordeaux, UMR 5251, INRIA Bordeaux Sud-Ouest, MEMPHIS team, F-33400 Talence, France
Email address: afaf.bouharguane@math.u-bordeaux.fr

Univ. Bordeaux, CNRS, Bordeaux INP, IMB, UMR 5251, F-33400 Talence, France
Email address: stephane.brull@math.u-bordeaux.fr